Adaptivity for the Lattice-Boltzmann Method

Project No 03 *DOM* 1 *FH* supported by bmb+f, Bundesministerium für Bildung und Forschung

1 Introduction

One of the projects at the Fraunhofer ITWM is the development of a software package,*ParPac*, whose purpose focuses on the simulation of filling casting molds. The core routine is a solver of the *incompressible Navier-Stokes* equation

$$\begin{aligned}\partial_t\mathbf{u} + \mathbf{u}\cdot\nabla\mathbf{u} &= -\nabla p + \nu\Delta\mathbf{u}\\ \operatorname{div}\mathbf{u} &= 0\\ \text{initial condition:}\quad \mathbf{u}|_{t=0} &= \mathbf{u}_0\\ \text{boundary condition:}\quad \mathbf{u}|_{\partial\Omega} &= \dots\end{aligned}$$

describing the motion of fluids inside a flow domain Ω. The velocity field $\mathbf{u}$ and the kinematic pressure p are unknown functions of time and space. ν denotes the *kinematic viscosity* as the only material parameter entering this model.
ParPac is based on the *Lattice-Boltzmann* method (LBM). Unlike FEM and FVM the primary unknowns are not the physical quantities but model variables, which are interpreted as particle densities or particle *populations*.

Adaptivity has turned out as a useful technique in order to make standard methods more efficient. The idea is to refine the discretization only locally in subregions with large numerical error or fine structured geometry.

The classical LBM works with a quadratic or cubic grid. In contrast to unstructured grids a local refinement is not possible. Alternatively, one can try to couple grids with different spacings.

On this poster we present some of our preliminary results of how to deal with adaptivity for the LBM, i.e. the problem of grid coupling and error estimating.

2 The LB Method

Consider the *Boltzmann equation* for the particle distribution function $f : T\times\Omega\times\mathbb{R}^3 \to \mathbb{R}_0^+$ with $f = f(t,\mathbf{x},\mathbf{v})$

$$\partial_t f + \mathbf{v}\cdot\nabla_{\mathbf{x}} f = Q(f,f)$$

Linearize collision operator: $Q(f,f) \quad\to\quad \mathbf{A}\cdot(f - f^{eq})$
Discretize the velocity space: $\mathbf{v}\in\mathbb{R}^3 \quad\to\quad \{\mathbf{c}_0 \dots \mathbf{c}_{N-1}\}$

Ingredients	Example: Incompressible D2Q9 LBGK
velocity space	$\mathbf{c}_k = c\,\mathbf{e}_k = c\,(\cos((k-1)\pi/4), \sin((k-1)\pi/4))$ for $k = 1 \dots 8$, $\mathbf{c}_0 = \mathbf{e}_0 = \mathbf{0}$ grid speed: $c = \frac{\delta s}{\delta t}$
primary variables	$F_k(t,\mathbf{x}) = F(t,\mathbf{x},\mathbf{c}_k)$, $\mathbf{F} = (F_0 \dots F_8)^t$
discretizing grid	uniform grid of equally sized squares with grid space δs, $\delta\mathbf{x}_k = \mathbf{e}_k\delta s$, time step δt
physical quantities	0th moment: $r = \sum_k F_k$, pressure: $r = 1 + 3c^{-2}p$, velocity: $\mathbf{u} = \sum_k F_k\mathbf{c}_k$
equilibrium	$\mathcal{E}_k(r,\mathbf{u}) = w_k r + w_k\left(\frac{3}{c}\mathbf{e}_k\cdot\mathbf{u} + \frac{9}{2c^2}(\mathbf{e}_k\cdot\mathbf{u})^2 - \frac{3}{2c^2}\mathbf{u}\cdot\mathbf{u}\right)$
weight factors	$w_0 = \frac{4}{9}$ $w_{1;3;5;7} = \frac{1}{9}$ $w_{2;4;6;8;} = \frac{1}{36}$
relaxation matrix & physical parameter	BGK model: $\mathbf{A} = -\frac{1}{\tau^*}\mathbf{I}$ $\tau := \frac{\tau^*}{\delta t}$ viscosity $\leftrightarrow$ relaxation time: $\nu = \frac{(2\tau-1)}{6}\frac{\delta s^2}{\delta t}$

The *Lattice-Boltzmann equation* is an explicit (i.e. implies no solving of linear systems) finite difference discrtization of the finite discrete velocity BGK Boltzmann equation:

$$F_k(\mathbf{x}+\delta\mathbf{x}_k, t+\delta t) = F_k(\mathbf{x},t) - \tfrac{1}{\tau}\Big(F_k(\mathbf{x},t) - \mathcal{E}_k\big(r(\mathbf{x},t),\mathbf{u}(\mathbf{x},t)\big)\Big)$$

Algorithmically, LBM comprises essentially two steps: the computation of the RHS of the LB equation at all nodes is called *collision* whereas *propagation* refers to the updating of populations, i.e. the shifting of collision products to neighbor nodes.

3 Scaling

Motivated by an asymptotic analysis, two scalings are introduced relating the spatial and temporal discretization increments:

acoustic scaling	diffusive scaling
$\delta s = \delta t \quad\Rightarrow\quad c := \frac{\delta s}{\delta t} = 1$	$\delta s = \delta t^2 \quad\Rightarrow\quad c := \frac{\delta s}{\delta t} = \frac{1}{\delta s}$

We have observed, that acoustic scaling may fail with large viscosities. 1D LBGK-Example: *Flow induced by oscillating wall.*

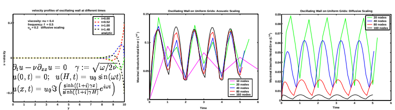

various flow profiles *acoustic scaling: l^∞ error* *diffusive scaling: l^∞ error*

The acoustic scaling enjoys much popularity in engineering. However, a thorough analysis confirms that not the acoustic but the diffusive scaling leads asymptotically to the incompressible Navier-Stokes equation.

4 Grid Coupling

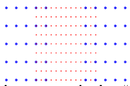

Some populations at the interface nodes are not reoccupied by the propagation step. If two neighboring subgrids overlap in a narrow zone, these unknown populations might be "refilled" by interpolating them from known populations of the adjacent subgrid. Unfortunately, this will not work directly. Diffusive scaling implies different particle speeds c on grids with unequal spacing. As populations depend on the abruptly changing c (cf. equilibrium in sec. 2), they expose also a discontinuous behavior which contradicts the implicit continuity assumption of interpolation. Moreover, it is not possible to calculate the populations from the physical quantities, since this leads either to singular or under-determined systems.
The way out is to enlarge the space of physical quantities by appropriately chosen moments of $\mathbf{c}$ w.r.t. to the populations. Like the physical quantities, these higher order moments must be asymptotically grid independent. For two adjacent subgrids A, B the transformation of populations takes then the form

$$\mathbf{F}_B = M^{-1}(c_B)\ \underbrace{M(c_A)\ \cdot\ \mathbf{F}_A}_{c\ \text{indep.moments}}$$

where M denotes the invertible mapping from the population into the moment space.

5 Applications

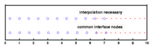

For the computation of the moments all populations are necessary. If an interface node coincides with a regular node of the adjacent subgrid, the moment transformation can be applied directly, otherwise the populations of the adjacent grid have to be interpolated in this interface node before they can be transformed.

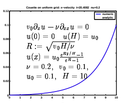

Grid coupling is first tested with stationary parallel shear flows. The populations are initialized by the equilibrium corresponding to the analytic solution. Because of initial layers, several iterations have to be performed before the scheme yields stationary populations. The first example of *Couette flow with constant cross flow* suggests, that apart from special situations higher order spatial interpolation will be necessary to avoid spoiling effects by the coupling.

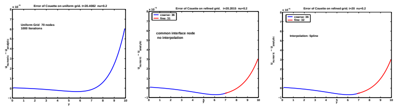

uniform grid *common interface node* *spline interp.*

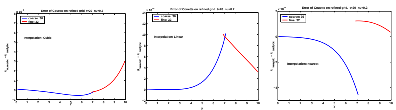

cubic interp. *linear interp.* *nearest interp.*

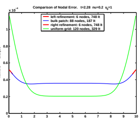

This figure shows the nodal error of a Poiseuille flow simulation. In order to decrease the error caused by the quite crude bounce-back boundary conditions, the grid is refined near the walls. For comparison the green curve represents the nodal error on an uniform grid. The numerical effort can be estimated by multiplying the number of grid nodes with the number of performed iterations. Note, that one iteration on the bulk patch corresponds to four iterations on the refined side patches due to diffusive scaling. Effort ratio: 25432 (adaptive) $\leftrightarrow$ 39480 (uniform).

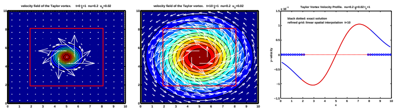

Taylor vortex $t = 0$ *Taylor vortex $t = 10$* *cross-section of x-vel. $t = 10$*

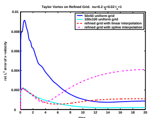

The Taylor vortex provides as an analytic solution of the 2D Stokes equation a suitable benchmark for local grid refinement. Due to viscosity the concentrated vortex is quickly smeared out; since the simulation uses a fixed domain the exact solution is prescribed at the boundary (bounce-back + velocity correction term). The relative L^1 error of the x-component of velocity (which is by reasons of symmetry equal the y-component error) is compared between a locally refined grid and two computations on uniform grids (global coarse=blue; global fine=cyan). Inside the red-framed area the grid spacing is halved; the computation is done utilizing spline (red) and linear (magenta) spatial interpolation.

6 A Model Problem

For the examination of adaptive error control for Lattice-Boltzmann methods the onedimensional Ruijgrok-Wu model

$$\begin{aligned}\partial_t u + \frac{1}{\epsilon}\partial_x u &= -\frac{\lambda\omega}{\epsilon^2}(u-v),\\ \partial_t v - \frac{1}{\epsilon}\partial_x v &= \frac{\lambda\omega}{\epsilon^2}(u-v)\end{aligned}\tag{1}$$

with $\lambda > 0$ and $\omega\in(0,1)$ is considered. In the limit ϵ to zero the mass density $\rho^\epsilon := u + v$ converges towards a solution ρ of the heat equation

$$\begin{aligned}\partial_t\rho &= \frac{1}{2\lambda\omega}\partial_x^2\rho \quad \text{in } (0,T)\times(a,b),\\ \rho(0,\cdot) &= \rho_0(\cdot) \quad \text{in } (a,b),\\ \rho(\cdot,a) &= \rho_a(\cdot), \quad \rho(\cdot,b) = \rho_b(\cdot) \quad \text{in } (0,T).\end{aligned}\tag{2}$$

Initial and boundary conditions for (1) are determined by data for (2). Adding a quadratic term to the right hand side of (1) leads to the viscous Burgers' equation as limit equation.
Discretization is done by the Lattice-Boltzmann type scheme

$$\begin{aligned}U_{l+1}^{k+1} - U_l^k &= -\omega(U_l^k - V_l^k),\\ V_{l-1}^{k+1} - V_l^k &= \omega(U_l^k - V_l^k)\end{aligned}\tag{3}$$

with piecewise constant functions in space and time and appropriate boundary and initial conditions, uniform gridspacing h and timestep $\tau := \lambda h^2$. This scheme is asymptotically consistent to the heat equation with viscosity $\nu = (1-\omega)/(2\lambda\omega)$ but not consistent to (1). An analogous situation is given in the BGK model.
Discretization (3) obeys the stability estimate

$$\begin{aligned}\|U_h(t_N)\|^2 + \|V_h(t_N)\|^2 + 2\,\frac{\omega}{\tau}\int_0^{t_N}\|U_h - V_h\|^2&\\ \le \|U_h(0)\|^2 + \|V_h(0)\|^2 + C(\rho_a,\rho_b)&.\end{aligned}$$

This provides an a priori error estimate of second order (due to superconvergence) for the errors

$$\begin{aligned}e_\rho &:= \rho - (U_h + V_h),\\ e_j &:= \frac{h}{2\omega}\partial_x\rho - (V_h - U_h)\end{aligned}$$

in the nodal norm $\|\cdot\|_D$ on uniform grids

$$\|e_\rho(T)\|_D + \|e_j(T)\|_D \le \|e_\rho(0)\|_D + \|e_j(0)\|_D + h^2K(\rho).$$

with constants depending on higher order derivatives of the solution of the limit equation. In problems without boundaries these expressions are bounded by initial data for U_h and V_h.
An a posteriori estimate in the L^2-norm is given by

$$\|e_\rho(T)\| + \|e_j(T)\| \le \|e_\rho(0)\| + \|e_j(0)\| + hK^{\text{posteriori}} + h^2K$$

with a constant $K^{\text{posteriori}}$ depending on discrete derivatives of U_h and V_h in space and time direction.

Quadratic convergence for a test problem.
$\rho(t,x) = e^{-\pi^2\nu t}\sin(\pi x)$ in $(0,1)$, $\nu = 0.1$, $\omega = 0.7$, $T = 0.5$.

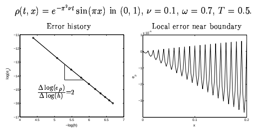

$N = 80, 160, 240, \dots, 800$ gridpoints. Superconvergence, $N = 100$.

Quadratic convergence for fixed endtime is also observed on non-uniform grids. Bisection of the gridspacing raises computational effort by a factor of 8 due to the space time coupling. Refining areas of relative width μ reduces the computational effort by the factor of μ compared to the effort needed to reach the same accuracy on uniform grids. LB methods on nonuniform grids end up with problems at the grid intersections (e.g. scaling, data interpolation). Reasonable results have only be obtained by using overlapping grids. The treatment of overlapping grids in higher dimensions is a demanding task.

Contact:

Project leader	Prof. Dr. W. Dörfler, FB Math., Uni KA	doerfler@math.uni-karlsruhe.de
Collaborator	Dipl.-Phys. M. Rheinländer, Fraunhofer ITWM KL	rheinlaender@itwm.fhg.de
Collaborator	Dipl.-Math. J.-P. Weiß, FB Math., Uni KA	weiss@math.uni-karlsruhe.de
ParPac develop.	Dr. K. Steiner, Dr. P. Klein, Fraunhofer ITWM KL	steiner@itwm.fhg.de klein@itwm.fhg.de
Industr. partner	Dr. W. Schäfer, MAGMA	schaefer@magmasoft.de

Background Pictures:
section 1: diffusor element of a power plant turbine (Heger-Guss)
section 2: discrete velocities of the D3Q15 model
section 4: stream lines of the driven cavity (Re 7000) - LB simulation

Layout: M. Rheinländer